



The metabolism of [^{14}C]-zibotentan (ZD4054) in rat, dog and human, the loss of the radiolabel and the identification of an anomalous peak, derived from the animal feed

Eva M. Lenz*, Alison Kenyon, Scott Martin, Dave Temesi, Jacqueline Clarkson-Jones, Helen Tomkinson

AstraZeneca Pharmaceuticals, Clinical Pharmacology and DMPK, Mereside, Alderley Park, Macclesfield SK10 4TG, United Kingdom

ARTICLE INFO

Article history:

Received 2 December 2010

Received in revised form 2 February 2011

Accepted 3 February 2011

Keywords:

Zibotentan
Metabolite-identification
Species differences
Loss of radiolabel
Isoflavones

ABSTRACT

This paper presents an overview of a cross-species investigation of the metabolic fate of [^{14}C]-zibotentan (ZD4054), with particular focus on the main analytical challenges encountered during the study. A combination of detection methods were used including HPLC coupled to UV, RAD and/or MS(MS), and ^1H NMR spectroscopy. The objective was to characterise and identify the major metabolites found in the circulation and excreta of rat and dog for comparison with those produced in human. Initial investigations in rat, using [^{14}C]-labelled zibotentan positioned on the oxadiazole ring and HPLC–UV–RAD analysis, revealed seven labelled resolved metabolite peaks. Parallel analysis by HPLC–UV–MS (with in-source fragmentation) uncovered two additional metabolites, indicating loss of the radiolabel during biotransformation. Hence, in subsequent studies in rat, dog and human, dual-radiolabelled zibotentan was employed with the ^{14}C -label positioned on the pyridine ring, which was shown to be less prone to metabolism. A total of 12 metabolites were found in the excreta and plasma in all species. One of these metabolites was found in the circulation in humans, which warranted further investigations. Characterisation of the isolated human circulating metabolite by ^1H NMR was complicated by the co-extraction of a matrix component with a similar UV-chromophore to zibotentan, which was identified as daidzein, an isoflavone derived from the animal feed.

© 2011 Elsevier B.V. All rights reserved.

1. Introduction

ZibotentanTM (AstraZeneca ZD4054, Fig. 1) is a specific endothelin A receptor (ET_A) antagonist, which is being developed for the treatment of castration-resistant prostate cancer (CRPC). With prostate cancer being the most common solid malignancy in men, and treatment options limited once the disease progresses to androgen independency, zibotentan represents a potential alternative therapy for patients with CRPC [1–7]. The compound is also currently investigated for the treatment of other cancer types, e.g. a phase II study is currently underway investigating its effectiveness in ovarian cancer [8,9]. The comparison of the full metabolite profiles derived from clinical and preclinical studies enables the identification of human specific and disproportionate drug metabolites which can profoundly affect the development of drugs [10,11]. Whilst most of the quantitative metabolite profiling work for [^{14}C]-zibotentan is covered in related publications [12,13], the main objective of this paper was to identify and provide a full structural characterisation of the major metabolites (>5% of administered

radioactive dose) found in the circulation and excreta of the pre-clinical species, rat and dog, and human (human volunteers).

On administration to these species during early development, [^{14}C]-zibotentan was found to be extensively metabolised. In total, 12 metabolites (labelled P1–P12) were identified in rat, dog and man, together with parent, which represented the major peak in the plasma profiles in all the species.

Whilst parent and metabolites P3 and P4 were identified in the urine and faeces samples in all the species investigated, metabolites P6, P8 and P9 were only detected in rat and human excreta.

Metabolites P8 and P9 were initially unaccounted for in the HPLC–UV–RAD trace owing to the fact that they had lost their oxadiazole radiolabel (Fig. 1A) during biotransformation.

The fact that the ^{14}C -radiolabelled oxadiazole ring was directly involved in the metabolism prompted the synthesis of a double-labelled equivalent (with the labels positioned on the pyridine ring, Fig. 1B) and the repetition of the metabolism studies.

Thus, metabolites P8 and P9 were subsequently confirmed and quantified in the repeat double-labelled study by HPLC–UV–RAD and HPLC–MS.

The remaining metabolites (namely P1, P2, P5, P7, P10, P11 and P12) were outside the scope of this paper, based on their low concentrations (<5% of dosed radioactivity).

* Corresponding author. Tel.: +44 1625 514653; fax: +44 1625 516962.
E-mail address: eva.lenz@astrazeneca.com (E.M. Lenz).

The identity of metabolite P6, however, was of particular interest, as it was the sole circulating metabolite in human plasma. Whilst isolating metabolite P6 from rat urine, an additional component was observed in the ^1H NMR spectrum, which required further evaluation, as it appeared compound related at first glance. This co-eluting compound was identified as an excreted product derived from the animal feed. It was identified as the flavonoid, daidzein based on its accurate mass and fragmentation data, and ^1H NMR spectroscopic evidence.

In this paper, we describe in detail the structure elucidation work and the learning derived from the earlier studies, with particular emphasis on the experimental design. Metabolic loss of radiolabel during the early single-labelled studies, coupled with limited MS fragmentation and interference from animal feed, has presented us with many challenges, despite the range of analytical techniques available, such as HPLC (analytical and semi-prep) coupled to UV, RAD and MS(MS), and ^1H NMR spectroscopy.

2. Methods and materials

2.1. Chemicals and materials

The reference standard, [^{14}C]-ZD4054, 3-methoxy-5-methyl-2-({2-[4-(1,3,4-oxadiazol-2-yl)-phenyl]-3-[2,6- ^{14}C] pyridyl} sulfonamido) pyrazine, with a radiochemical purity of >98% was synthesised by Isotope Chemistry Group, DMPK, AstraZeneca UK Ltd. and stored at -80°C in the dark until required.

A series of potential synthetic metabolites were manufactured by the Chemistry Department, AstraZeneca UK Ltd., based on intermediates produced during the synthesis of zibotentan, such as the amino pyrazine moiety and the biaryl acid, of which only the biaryl acid (P8) was detected *in vivo*. Novacta Biosystems Ltd. generated the microbial metabolites P3 and P4, which were structurally characterised within AstraZeneca UK Ltd. Synthetic daidzein was acquired from Sigma–Aldrich (Poole, UK).

Fisher Scientific (Loughborough, UK) supplied acetonitrile (ACN) and methanol (MeOH). All other chemicals were purchased from commercial suppliers and were of analytical grade or the best equivalent. The deuterated NMR solvents were supplied by Sigma–Aldrich (Poole, UK).

2.2. Species, dosing and dose formulations

All animal experiments were conducted in GLP compliant facilities, with food (a standard SDS diet) and water available *ad libitum* to the rats. Dogs were offered 400 g of standard formulation food *ca.* 30 min before dosing and daily thereafter, with water supplied *ad libitum*.

Rats (Wistar, $n=6$, three male, three female) received a dose of singly labelled [^{14}C]-zibotentan at 10 mg/kg orally and 5 mg/kg intravenously (*iv*), while in the repeat study, double-labelled [^{14}C]-zibotentan was dosed at 5 mg/kg (oral) and 3 mg/kg (*iv*), and urine, faeces and plasma were collected.

Dog (Beagle, $n=3$, male dogs only) were initially dosed at 1 mg/kg, for both oral and *iv*, with single-labelled [^{14}C]-zibotentan. In the repeat study, the dogs ($n=6$, three male, three female) received an oral dose of double-labelled [^{14}C]-zibotentan of 1 mg/kg, and urine, faeces and plasma were collected.

Humans received initially a 60 mg dose orally ($n=6$, all male) of unlabelled zibotentan (data not shown). In a second study human volunteers ($n=6$, three male, three female) received an oral dose of double-labelled [^{14}C]-zibotentan of 15 mg, and urine, faeces and plasma were collected.

The oral dose for both rat and dog was formulated as a nominal 1 mg/mL suspension in 0.5% (w/v) hydroxypropyl methylcellulose

(HPMC) containing 0.1% aqueous polysorbate 80. The intravenous dose was formulated as a nominal 1 mg/mL (for dog) and 2 mg/mL (for rat) solution in polyethylene glycol (PEG) 400:phosphate buffered saline solution (PBS) (50:50). Both dose formulations were prepared at Alderley Park, AstraZeneca UK Ltd., and were used within their shelf-life and were found to be radiochemically pure, homogeneous and within 5% of their target concentration. Humans received their dose as an aqueous suspension (15 mg/150 mL water).

2.3. Sample preparation

The samples of plasma, urine and faeces from rat, dog and human were prepared as detailed below.

Rat: Plasma samples (0–24 h) were pooled using a set volume of each sample (volume = 200 μL), by dose group and by sex, to yield a total of four pools.

Extracts of each pool were produced by mixing with ACN (plasma:ACN, 1:3, v/v), followed by centrifugation at approximately $3000 \times g$. The supernatant was decanted and the radioactivity assessed by liquid scintillation counting (LSC). A mean extraction efficiency of 87.4% was calculated. Extracts were concentrated under a stream of oxygen free nitrogen (OFN) until a small volume remained.

Urine samples (0–48 h) were pooled by sex and dose group, by using approximately 10% by weight of each rat urine sample to yield a total of four urine pools. Each pool was assessed for radioactivity by LSC. Samples were centrifuged (at approximately $3000 \times g$) to remove any particulate matter prior to chromatography.

Faeces homogenate samples were pooled using 10% (by weight) of each sample to yield one male and one female pool (0–48 h) for each dose group (oral and *iv*). Faecal homogenate pools were extracted with ACN (faeces homogenate:ACN, 1:3, v/v), mixed for approximately 2 h and centrifuged at approximately $1900 \times g$. The supernatant was decanted and the resulting faeces extract was assessed for radioactivity by LSC. The mean extraction efficiency of the faeces extract was 87.4%. Each pool was concentrated under a stream of OFN until a small volume remained.

Dog: Plasma samples (0–24 h) were pooled using a set volume of each sample (2 mL aliquots), by sex, to give two pools. Extracts of each pool were prepared as described above. A plasma extract with an extraction efficiency of 93.2% was selected and analysed by HPLC–MS.

For each dog, urine samples (0–48 h) were pooled using 5% by weight and processed as described above.

Aliquots of faecal homogenates (0.5% by weight) were pooled by animal to give six 0–48 h samples (as most of radioactivity was excreted in 48 h) and extracted as described above. A mean extraction efficiency of 86.9% was achieved.

Human: Plasma (0–24 h) was pooled (by taking 5 mL aliquots from each volunteer) and extracted as detailed above. Following LSC to assess extraction efficiency (89.9%), the extracts were dried under OFN prior to HPLC.

Urine samples were pooled (by taking approximately 1% by weight of each urine sample) to generate individual 0–72 h samples for six subjects and then centrifuged, as described above. The resulting supernatant was snap-frozen in liquid nitrogen, freeze-dried and each dried pool was reconstituted in a small volume of deionised water to concentrate the sample.

Faecal samples were pooled for each volunteer (0–120 h) using 4% by weight to yield six pools. Extraction was carried out as stated above, three times successively, per sample. The mean extraction efficiency was calculated as 76.2%.

The centrifuged urine samples were injected directly onto the HPLC–UV–RAD or HPLC–MS, while faecal and plasma extracts were reconstituted in deionised water prior to analysis.

2.4. Determination of radioactivity concentrations

Assessment of radioactivity by LSC was carried out throughout the course of these studies. Duplicate sample aliquots were weighed, made up to volume (1 mL) with deionised water, and 10 mL of Packard Ultima Gold Scintillant was added.

Radioactivity was determined using a Model 2100TR (PerkinElmer Life Sciences, UK) liquid scintillation analyser. Quench correction was checked using quenched radioactive reference standards. Samples were counted to a sigma 2 counting error of 0.5% or for 10 min. Appropriate liquid scintillant blanks were counted to establish background levels of radioactivity. Blank counts were subtracted from sample counts and subsequently quench corrected.

2.5. Chromatographic conditions, instrumentation and data capture

2.5.1. Metabolite profiling

Metabolite profiles of prepared plasma, urine and faecal homogenate samples were generated by high performance liquid chromatography coupled with ultraviolet and radiochemical detection (HPLC–UV–RAD). Selected samples were also analysed by HPLC–MS. Isolation of individual metabolites for structural confirmation by ^1H NMR spectroscopy was carried out using the rat urine samples, exclusively.

2.5.2. Analytical acetonitrile HPLC system

Both metabolite profiling and HPLC–MS investigations utilised the conditions as outlined here.

UV detection at a fixed wavelength of 259 nm was used alongside each HPLC system. HPLC pumps used for metabolite profiling and identification were PerkinElmer 200 Series. Two types of UV detector were used, the Shimadzu UV–Vis 10A and the Jasco 2075 plus.

The chromatographic separations were carried out at room temperature on a Zorbax Rx–C₁₈ column (25 cm × 0.46 cm) with a mobile phase system consisting of solvent A (water:formic acid, 1000:2, v/v) and B (ACN:formic acid, 1000:2, v/v), with a flow-rate of 1.5 mL/min. A linear gradient was employed from 5 to 30% B over 20 min, held at 30% B for a further 10 min and increased to 80% B in 5 min, before re-equilibration and injection of a new sample.

Packard 500TR Radiochemical detectors with liquid flow cells (scintillant flow rate 3 mL/min using Ultima Gold Scintillant from PerkinElmer Instruments) were used in conjunction with HPLC instruments for metabolite profiling. HPLC–UV–RAD data were collected and analysed using Packard Flo one software (version 1/3.60).

Metabolite isolation was performed using the chromatographic conditions as detailed in the following sections.

2.5.3. Preparative acetonitrile HPLC system

The preparatory ACN system used the same eluents and equipment as detailed in the analytical ACN system; however, here, a preparative column (Hichrom HIRB–250004, 13 cm × 3 cm) was used with a flow rate of 5 mL/min. The gradient was also adjusted such that after keeping B at 20% isocratically for 10 min, a linear gradient was employed from 10 to 15 min increasing B to 30%, which was held at 30% B for a further 8 min and finally increased to 70% B in 1 min, before re-equilibration and injection of a new sample.

2.5.4. Preparatory methanol HPLC system

The preparatory MeOH system used the same column and equipment as the analytical ACN system detailed above with the exception of the eluents and HPLC gradient. Again, a flow rate of 5 mL/min was employed, with a mobile phase comprising solvent A

(water:formic acid, 1000:2, v/v) and B (MeOH:formic acid, 1000:2, v/v) at an initial mobile phase concentration of 8% B. A linear gradient was then employed from 8 to 38% B over 20 min, held at 38% B for a further 10 min and increased to 70% B in 1 min, before re-equilibration and injection of a new sample.

2.5.5. Isolation of individual metabolites (P3 and P4)

Urine samples from the single oxadiazole labelled rat study (0–6 h urine) were used as a source of the metabolites P3 and P4 for isolation and characterisation by ^1H NMR analysis. Several approaches to isolate sufficient material were taken. In brief, the isolation of metabolite P4 was conducted in three stages. All samples underwent stage 1, whilst some underwent stage 2 or 3 or both, prior to ^1H NMR analysis.

Stage 1: Samples were subjected to HPLC using both the preparative and analytical ACN systems, as described above. Fractions containing P3 or P4 were collected manually, pooled, concentrated under OFN and freeze dried.

Stage 2: Some pooled samples underwent solid phase extraction (SPE) using C18 Isolute cartridges eluted with 30:70 (v/v) MeOH:water. These samples were then concentrated under OFN, freeze dried and submitted for HPLC–MS analysis using the analytical ACN HPLC method.

Stage 3: Samples were subjected to further HPLC–fraction collection using the MeOH preparatory system. Fractions containing P4 were collected manually, pooled, concentrated under OFN and freeze dried.

2.5.6. Isolation of metabolite P6

Metabolite P6 was isolated from pooled rat urine (from the single-labelled study) by taking approximately 30% by weight from each 0–6 h rat urine sample. The quantity of P6 contained was assessed by LSC, in order to determine the dpm, and by HPLC–UV–RAD analysis.

The pooled rat urine sample was subjected to HPLC, using the analytical ACN HPLC method, and serially fractionated using the methods detailed below. Once isolated, fractions containing metabolite P6 were submitted for analysis by ^1H NMR and ion trap–MS to confirm the structure.

Fraction collection (1): The 0–6 h rat urine pool was separated utilising the chromatographic conditions as detailed in the analytical ACN system. Fractions were collected at 1 min intervals into freshly washed LSC vials using a Pharmacia LKB Superfrac automated fraction collector. The process was repeated serially into the same set of vials. The presence of metabolite P6 in fraction (1) was determined by HPLC–UV–RAD and HPLC–MS analysis using the chromatographic and MS set up as detailed. Fraction (1) was concentrated under a stream of OFN until only a small volume remained.

Fraction collection (2): The concentrated fraction was then further purified via the analytical ACN HPLC system (with the exception that formic acid was omitted from the mobile phase) and the UV–peak (with the retention time characteristic of P6) was collected manually over two fractions, A and B. The presence of metabolite P6 in the fractions was quantified by LSC and verified by HPLC–UV–RAD and HPLC–MS analysis. The individual fractions were concentrated under a stream of nitrogen, followed by freeze-drying. The fractions were analysed initially by HPLC–MS, then QTOF–MS, and finally ^1H NMR spectroscopy.

2.5.7. Characterisation by HPLC–MS

In general, most of the structural characterisation (on parent and metabolites P3, P4, P8, P9 and P6) was carried out using the single quadrupole Waters ZQ mass spectrometer. The Waters Q–Tof 2 mass spectrometer instrument was used to mass measure and

predict the elemental composition of the unknown co-extracted component in fraction A, identified as daidzein, the analysis of which was later repeated to a higher mass accuracy on the LTQ-Orbitrap in urinary daidzein. The LTQ-Orbitrap was also used to reassess the parent compound and further isoflavones contained in control rat urine.

Thus, initial metabolite identification experiments were performed using a PerkinElmer 200 Series HPLC system equipped with UV-detection and coupled to a Waters ZQ mass spectrometer with integral electrospray ionisation (ESI) source (Waters Corporation, Milford, USA), with the HPLC-conditions as outlined in the analytical ACN HPLC system section. Data were acquired in full scan acquisition mode (20–800 Da) at a scan speed of 2 s and processed using Masslynx version 3.5. Alternating low–high cone voltage settings were 25 V and 50 V, respectively. The source, cone and desolvation temperatures were set at 120 °C, 520 °C and 300 °C, respectively. The desolvation and cone gases were set up at 460 L/h and 37 L/h, respectively.

The Waters Q-ToF 2 mass spectrometer (Waters Corporation, Milford, USA) was equipped with an ESI source, operating in positive mode, with data acquired at 1 scan per second. The source and desolvation temperatures were 120 °C and 350 °C, respectively. The desolvation and cone gases were set up at 750 L/h and 5 L/h, respectively. Full scan MS data were obtained in centroid mode over the mass range of 50–900 Da at a peak resolution of 7000 using alternating low (40 V) and high (80 V) cone volt switching to generate molecular ions and source induced fragments. Data were acquired using a continuous lock mass infusion to ensure mass stability. All ion spectra were collected using 10 V collision energy. Data acquisition and processing were handled by Masslynx version 3.5.

Daidzein (contained in rat urine), and further urinary isoflavones were analysed on a Waters Acquity UPLC–MS system equipped with a binary solvent manager, column oven, sample manager and DAD UV/visible detector (Waters Corporation, Milford, USA) linked to the mass spectrometer as described below. Separations were carried on a Kinetics 2.6 μ m core shell 100 mm \times 2.1 mm i.d. column (Phenomenex, Macclesfield, UK) maintained at 50 °C. The mobile phase consisted of eluent A (ammonium acetate 10 mM) and eluent B (methanolic ammonium acetate 10 mM). The elution profile described a linear gradient from 10% to 80% B from 0 to 8 min, followed by an isocratic hold at 95% B from 8 to 11 min, before re-equilibration (10% B, from 11 to 15 min). The flow rate was 0.5 mL/min, the injection volume was 20 μ L and DAD UV spectra were acquired from 190 to 330 nm. Eluent flow was introduced into the mass spectrometer *via* the LTQ divert valve at 1.0 min. The mass spectrometer was a LTQ-Orbitrap XL equipped with an ESI source (Thermo Fisher Scientific, Bremen, Germany), which was operated in positive mode. Source settings were: capillary temperature 350 °C, sheath gas flow 25, auxiliary gas flow 17 and sweep gas flow 5 (L/h), source voltage 3.5 kV, source current 100.0 μ A, capillary voltage 18 V and tube lens 75 V. Full scan MS data were obtained over the mass range 100–1000 Da at a peak resolution of 7500. Targeted MSMS experiments were acquired using HCD (collision cell) fragmentation, isolation width 2 Da, normalised collision energy 45 and activation time 30 ms. HCD fragment ions were monitored by the Orbitrap using 7500 resolution. LTQ and Orbitrap mass detectors were calibrated within 1 day of commencing the work using Proteomass LTQ/FT-Hybrid ESI positive mode calibration mix (Supelco, Bellefonte, USA). Data acquisition and processing were handled by Xcalibur software version 2.1.

2.5.8. Characterisation by ^1H NMR spectroscopy

Generally, individual metabolite peaks were isolated by HPLC, as outlined above, prior to investigation by ^1H NMR spectroscopy. All metabolites were reconstituted in 200 μ L D_2O and transferred into 2.5 mm i.d. microtubes prior to analysis.

^1H NMR spectroscopy was performed on a Bruker DRX500 NMR spectrometer operating at 500.13 MHz resonance frequency. ^1H NMR data were collected and analysed using XWIN-NMR version 2.6. Typically the ^1H NMR spectra were acquired with solvent suppression at the water frequency. Data were acquired into 65k data points over a spectrum width of 9980 Hz at a constant temperature of 300 K. Depending on concentration of the metabolites, spectra were recorded with 512–4096 scans.

3. Results and discussion

3.1. Metabolite profiles of [^{14}C]-zibotentan in rat, dog and human samples

Metabolite profiling was performed using HPLC–UV–RAD, the profiles of which also provided the quantitative data to calculate the proportion of dose represented by each metabolite. Subsequent metabolite characterisation was performed by HPLC–MS and, following off-line isolation by HPLC, by ^1H NMR spectroscopy.

Although some of the quantitative work is discussed in detail by Clarkson-Jones et al. [12,13] for both human and pre-clinical species (mouse, rat and dog, bile-duct cannulated and intact), dosed with double-labelled [^{14}C]-zibotentan, this paper serves to summarise the mass balance and metabolite profiling data, and most importantly, demonstrate the learning from the earlier investigations.

Hence, the findings from the initial single-labelled studies are presented, highlighting the detection of radioactivity in the expired air in rats, as well as the identification of unlabelled metabolites in rat excreta, which provided the rationale for the repetition of the studies, using the double-labelled compound, in intact animals and humans.

Representative HPLC–RAD profiles of rat, dog and human urine as well as human plasma, following dosing of double-labelled [^{14}C]-zibotentan, are shown in Fig. 2, and the data for each species are discussed and summarised in the following paragraphs.

3.1.1. Rat

An excretion balance study was carried out initially with the single-labelled compound. In total, ca. 92% of the radioactivity of the oral dose was recovered from males and 99% from females. Recoveries from intravenous administration were similar with approximately 88% recovered from males and 97% from females. Following both oral and intravenous administration excretion was rapid with more than 74% of the dose being recovered in the first 24 h.

Metabolite patterns were similar following both oral and *iv* dosing, and although there were some quantitative differences, males and females excreted the same metabolites. There was no apparent inter-animal variation in the metabolite patterns from animals of the same sex.

There was, however, a distinct sex difference in excretion of [^{14}C]-zibotentan. Males had significantly higher levels of radioactivity in the faeces (and expired air). Thus, collections up to 48 h revealed, following the oral dose to males, a recovery of ca. 19% in urine, 64% in faeces, and 4.4% in expired air, and following *iv* dosing, 32% in urine, 45% in faeces and 8% in expired air. In females, the figures were 46% in urine, 44% in faeces and 2% in expired air following oral dosing, and 72% in urine, 14% in faeces and 3% in expired air, following *iv* dosing.

The sex difference was also observed in the quantities of parent compound and individual metabolites seen in the excreta profiles, with metabolism generally more pronounced in males (data not shown).

The relatively high level of radioactivity observed in expired air indicated that the position of the radiolabel was not metabolically

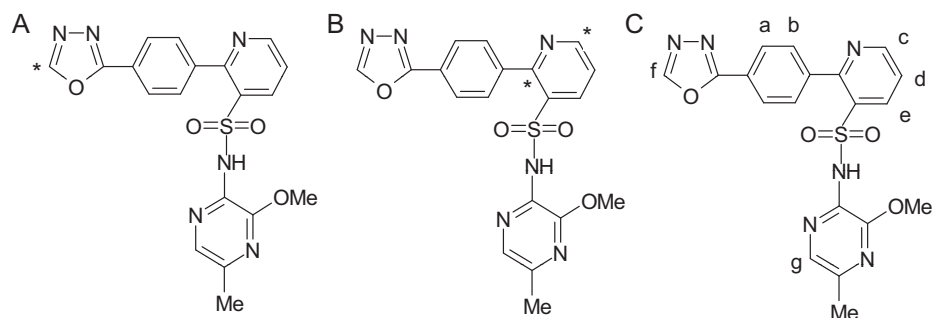


Fig. 1. The structure of [^{14}C]-zibotentan showing (A) the initial position of the radiolabel (*) and (B) the positions of the radiolabel in the pyridine ring in the repeat double-labelled study. The structure of [^{14}C]-zibotentan with the protons as labelled in the ^1H NMR spectra throughout the paper (C).

stable. This observation then led to the production of the double-labelled version of zibotentan and the repetition of the study.

Hence, as expected, the sex difference was also apparent in the repeat double-labelled study. The urine and faecal metabolite profiles showed that metabolism was generally higher in males than in females, particularly in the quantities of metabolite P4. Thus, in males, P4 accounted for 60% of the oral and 45% of the *iv* dose, whilst in females, the figures were 23% and 13%, respectively. Females excreted the majority of the dose as parent, accounting for 47% of the oral and 48% of the *iv* dose. In contrast, males excreted only 7% of the oral dose and 8% of the *iv* dose as parent.

In all rats the main component in the circulation was confirmed as parent, which accounted for approximately 83% and 90% of radioactivity following oral and *iv* dosing, respectively. Plasma was generally void of major circulating metabolites; however, metabolite P4 was observed in male rats only, following both dose routes, but only accounted for 2% of the radioactivity. Metabolite P6 was also observed at low levels (less than 1% of activity present) in the circulation of male rats following *iv* dosing.

Seven metabolite peaks were observed in urine and faeces using HPLC–UV–RAD and these were identified as peaks 1–7 (P1–P7) in the single-labelled study. The double-labelled repeat study additionally highlighted the presence of P8 and P9, minor metabolites present (at <4%) in the urine and faeces. Parent eluted at a retention time (RT) of 22.1 min while all of the metabolites, with the exception of P6, eluted before parent.

A summary of the key metabolites present in the HPLC–UV–RAD profiles from the double-labelled study is provided in Table 1A.

3.1.2. Dog

An excretion balance study was initially carried out with the single-labelled compound in male dogs only. In total, ca. 86% and 97% of the administered radioactivity was recovered during the collection period, following oral and *iv* dosing, respectively. Excretion was rapid with more than 96% of the recovered dose being eliminated within 48 h of administration. Urinary recoveries following *iv* dosing were higher than the ones following the oral route, as oral absorption was estimated at 66%. Expired air was not collected.

Metabolite profiles in urine and faeces extracts were found to be qualitatively similar following both oral and *iv* dosing to the male dogs, although the data were generally variable, as one dog was found to metabolise extensively. As a brief summary, the major peak in urine and faeces was from parent (representing approximately 30% and 50% in urine and ca. 9% and 3% in faeces, following oral and *iv* administration, respectively). Three other components (P4, P3 and P2) were also observed in the excreta. Metabolite P4 represented ca. 12% and 8% in urine and ca. 13% and 8% of the administered dose in faeces, following oral and *iv* dosing, respectively. P3 accounted for ca. 4% and 7% in urine but less than 3% and 1% in faeces, while P2 accounted for less than 1% of the dose in both urine and faeces, following oral and *iv* dosing, respectively.

Plasma contained one major peak consistent with parent (ranging from 63–80% and 80–87% following oral and *iv* dosing, respectively), whilst P3 and P4 combined account for less than 6% of the chromatogram radioactivity, following either dose route.

In the repeat double-labelled study, following oral dosing to male and female dogs, the metabolic profile was similar to that in the single-labelled study. Furthermore, no sex difference was observed in the excretion of metabolites.

Hence, ca. 40% of the dose was recovered as parent, the majority of this (ca. 37%) was recovered in urine. P4 accounted for approximately 12% in urine and 7% in faeces, and P3 for approximately 7% of the dose in, both urine and faeces. P2 represented less than 0.5% in urine and 3% in faeces. In all dogs, the main component in circulation was parent, accounting for approximately 92% of the circulating radioactivity, with both P3 and P4, representing ca. 5% of the chromatogram radioactivity.

A summary of the key metabolites present in the HPLC–UV–RAD profiles from the double-labelled study is provided in Table 1B.

3.1.3. Human

Following a single oral dose of double-labelled [^{14}C]-zibotentan to human volunteers, the resulting routes of excretion and metabolite profiles were similar for both male and female volunteers. There was little inter-individual variation in the range and quantity of the metabolites observed, as discussed in Ref. [13].

Clarkson-Jones et al. [13] showed that [^{14}C]-zibotentan was rapidly absorbed, with the maximum plasma concentration observed 1 h after administration. Excretion was rapid, with the majority of the dose being excreted in the urine (with a mean of 83%), whilst the remainder (approximately 10% of the dose) was eliminated *via* the faeces. Thus, the total recovery of radioactivity was high (with a mean of 93% over 5 days), with 78% of the dose being recovered within the first 24 h.

The major component in human plasma was parent compound, which accounted for approximately 80% of the circulating material over 24 h, together with metabolite P6, which was present at levels of approximately 4%. No other metabolites were observed in the human plasma over 24 h.

In human urine the main component observed was parent accounting for approximately 36% of the dose, whereas in faeces, parent compound was either absent or only detected at trace levels. In both human urine and faecal samples, P3 and P4 were the main metabolites observed, accounting for ca. 13% and 12% of the dosed radioactivity in urine, and approximately 2% of the dose, for both, in the faeces, respectively. In urine, P2 and P6 were also of note accounting for ca. 3% and 6% of the dose, respectively. All other metabolites accounted for less than 3% of the dose in urine and 1% of the dose in faeces. Both P8 and P9 were only present at trace levels (less than 1%) in urine and faeces.

Table 1

HPLC-peaks observed, following dosing of double-labelled [^{14}C]-zibotentan, in the (A) 0–48 h urine and faecal samples and 0–24 h plasma samples following oral (5 mg/kg) and intravenous (3 mg/kg) dosing to three male and three female rats. (B) 0–48 h urine and faecal, and 0–24 h plasma samples following oral dosing (1 mg/kg) to three male and three female dogs. (C) 0–72 h urine, 0–120 h faecal and 0–24 h plasma samples following a single 15 mg oral dose to healthy volunteers (male and female, $n = 3$ each).

Species	Dose route/sex/sample	HPLC peaks and retention times (min)							
		P2 12.5	P9 13.7	P3 15.1	P4 16.6	P5 18.0	P8 20.9	Parent 22.1	P6 23.6
(A) Rat	O/M/U	n/d	0.8	2.1	18.5	n/d	2.1	3.6	0.7
	O/F/U	n/d	n/d	1.8	7.8	n/d	1.4	40.9	5.1
	IV/M/U	n/d	0.7	1.6	16.7	n/d	1.8	6.1	6.7
	IV/F/U	n/d	n/d	3.2	5.4	n/d	1.0	47.5	2.3
	O/M/Fc	n/d	1.1	1.7	41.5	n/d	3.8	3.4	n/d
	O/F/Fc	n/d	0.4	0.9	15.6	n/d	2.1	5.6	1.0
	IV/M/Fc	n/d	0.7	1.1	28.6	2.0	2.7	1.6	1.0
	IV/F/Fc	n/d	0.2	0.4	7.3	2.3	1.2	0.7	0.1
	O/M/P	n/d	n/d	n/d	1.9	n/d	n/d	82.4	n/d
	O/F/P	n/d	n/d	n/d	n/d	n/d	n/d	84.5	n/d
	IV/M/P	n/d	n/d	n/d	2.0	n/d	n/d	89.9	0.8
	IV/F/P	n/d	n/d	n/d	n/d	n/d	n/d	90.6	n/d
	(B) Dog	O/M/U ^{6–48 h}	n/d	n/d	6.4	11.3	n/d	n/d	37.0
O/F/U		<0.5	n/d	7.4	12.3	n/d	n/d	36.6	n/d
O/M/Fc		1.0	n/d	6.4	6.9	n/d	n/d	3.2	n/d
O/F/Fc		4.6	n/d	8.3	5.9	n/d	n/d	1.5	n/d
O/M/P ^{6–24 h}		n/d	n/d	5.3	n/d	n/d	n/d	94.7	n/d
O/F/P		n/d	n/d	5.0	5.8	n/d	n/d	89.2	n/d
(C) Human		O/M/U	3.3	n/d	13.3	12.4	0.9	1.5	36.3
	O/F/U	3.4	n/d	12.9	12.2	1.5	n/d	35.5	4.6
	O/M/Fc	<1	<1	1.8	3.6	<1	<1	<1	n/d
	O/F/Fc	<1	<1	2.1	1.2	<1	n/d	n/d	n/d
	O/M/P	n/d	n/d	n/d	n/d	n/d	n/d	79.5	4.2
	O/F/P	n/d	n/d	n/d	n/d	n/d	n/d	81.1	4.4

Results expressed as percentage of dose, except for plasma, which is expressed as percentage of chromatogram.

n/d = not detected.

Mean of three animals/volunteers, unless stated otherwise.

Key—O: oral; IV: intravenous; M: male; F: female; U: urine; Fc: faeces; and P: plasma.

A summary of the key human metabolites present in the HPLC–UV–RAD profiles from the double-labelled study is provided in Table 1C.

In summary, during early development, when [^{14}C]-zibotentan was administered to rats, dogs and human volunteers, it was shown to be rapidly absorbed, with the majority of the radioactivity excreted within 24 h by rats and humans, and within 48 h by dogs.

Based on the data from the double-labelled studies (Table 1), parent compound accounted for ca. 80% and 89–95% of circulating radioactivity in humans and dogs, respectively, following oral administration, and for approximately 82–91% in rats, following oral and iv doses.

In the urine and faecal profiles of rats, a distinct sex difference was observed, with metabolism more extensive in males, an observation not made in dogs and humans. Hence, female rats excreted the majority of the dose as parent (ca. 48%), compared to ca. 8% in males. This phenomenon was also apparent in the preliminary single-labelled study, with the detection of radioactivity in the expired air (up to 8% in male rats, compared to 3% in females). Most importantly, however, the capture of expelled $^{14}\text{CO}_2$ indicated loss of the radiolabel as a consequence of biotransformation.

[^{14}C]-Zibotentan was found to be extensively metabolised. In total, 12 metabolites (P1–P12) were identified in rat, dog and human, none of which, however, unique to one species. Generally, the metabolite profiles from rat and human samples were more complex compared to those from dog. Parent and the major metabolites P3 and P4 were identified in the urine and faeces samples in all the species investigated, while P6, P8 and P9 were only detected in rat and human excreta. Metabolites P8 and P9 were initially unaccounted for in the HPLC–UV–RAD traces from rats following dosing of single-labelled [^{14}C]-zibotentan, owing to the fact that they appeared to have lost their radiolabel during bio-

transformation. P8 was solely identified in rat urine by HPLC–MS, based on a diagnostic fragment ion. P8 and P9 were later confirmed, characterised and quantified in the double-label repeat study, by HPLC–UV–RAD and HPLC–MS.

3.2. Structural characterisation of parent and metabolites

Metabolite characterisation was performed using a selection of HPLC–MS(MS) detectors. In general, the primary analyses were carried out on a single quadrupole mass spectrometer using alternating low–high cone voltage switching to facilitate in-source fragmentation. Accurate mass measurement and MSMS experiments were acquired on QTOF-MS and LTQ Orbitrap instruments on selected samples. Metabolites were uncovered using HPLC–UV–RAD in conjunction with MS mining techniques such as common fragment searching and ^{14}C isotope pattern matching. The fragment ion at m/z 139, representing the amino pyrazine ring, was particularly useful for identifying HPLC–MS components as being derived from [^{14}C]-zibotentan. Biotransformation characterisation was based on molecular ion and fragmentation information. Finally, once isolated, selected metabolites were analysed by ^1H NMR spectroscopy for their structural identification.

It should be noted that the LTQ Orbitrap work was limited to the identification of the feed contaminant, daidzein, and was also used to re-evaluate the fragmentation of parent.

3.2.1. Structural assignment of [^{14}C]-zibotentan parent

Drug metabolites generally contain common or similar structural motifs to the parent drug; hence, prior to the identification of the metabolites, the pure dosed compound was fully structurally characterised by HPLC–MS, with additional MSMS, and ^1H NMR spectroscopy. The resulting information helped to find and identify

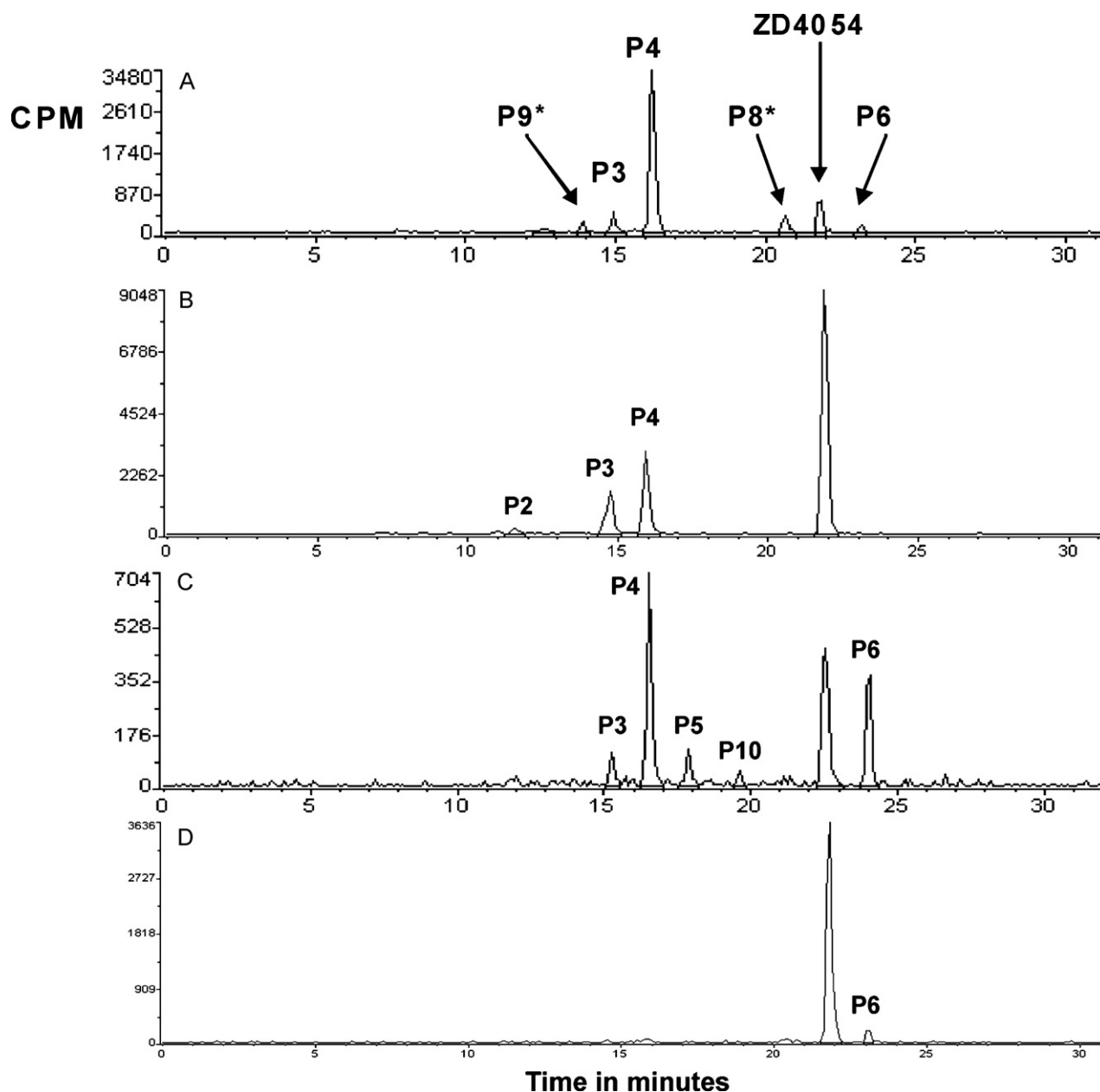


Fig. 2. Representative HPLC–RAD profiles of (A) rat urine (0–48 h pool), (B) dog urine (0–48 h urine pool), (C) human urine (12–24 h urine pool) and (D) human plasma (0–24 h pool), following dosing of double-labelled [^{14}C]-zibotentan. * P8 and P9 were unaccounted for in the single-label study, due to loss of the radiolabel.

diagnostic fragment ions and NMR signals in the complex biological samples.

The proposed fragmentation pattern for parent is shown in Fig. 3, and the ^1H NMR spectra of parent (in different solvents) are shown in Fig. 4.

[^{14}C]-Zibotentan (with a RT of approximately 22.1 min) yielded a protonated molecular ion $[\text{M}+\text{H}]^+$ of m/z 425 when analysed by HPLC–MS at the low cone voltage (25 V). The mass fragmentation patterns showed that ionisation at the high cone voltage (50 V) resulted in three key fragments, namely m/z 139 and m/z 237 (both odd electron ions) and m/z 361, following expulsion of the sulfone moiety. These fragment ions were deemed to be very unusual and hence were later confirmed by accurate mass (<3 ppm) MSMS on the LTQ Orbitrap, as shown in Fig. 3. The proposed expulsion of the sulfone moiety and subsequent rearrangement process is supported by mechanistic studies in previous work on sulfonamides by Wang et al. [14]. The characteristic isotope pattern was present

in all the fragments with the exception of the fragment of m/z 139, as the pyrazine ring did not contain the ^{14}C label.

Characterisation by ^1H NMR spectroscopy highlighted that [^{14}C]-zibotentan was exclusively suited to heavy water (D_2O), as all other solvents or solvent mixtures resulted in broadening of some of the signals, as shown in Fig. 4 (with proton peak labels as in Fig. 1C). Although the compound dissolved readily in all the solvents investigated, some solvents (especially ACN-d_3 or MeOH-d_4) caused severe loss of signal intensity and resolution, which could compromise data interpretation in subsequent metabolite identification work. Solvents, such as DMSO-d_6 and chloroform-d_3 , proved equally unsuitable. In the case of the $\text{ACN-d}_3/\text{D}_2\text{O}$ -mixture (50:50, v/v), a typical solvent system employed for on-line HPLC–NMR separations, this problem was further amplified. Hence, for the metabolites of interest, off-line isolation of the metabolites was required, followed by reconstitution in D_2O , in order to achieve reliable structural characterisation.

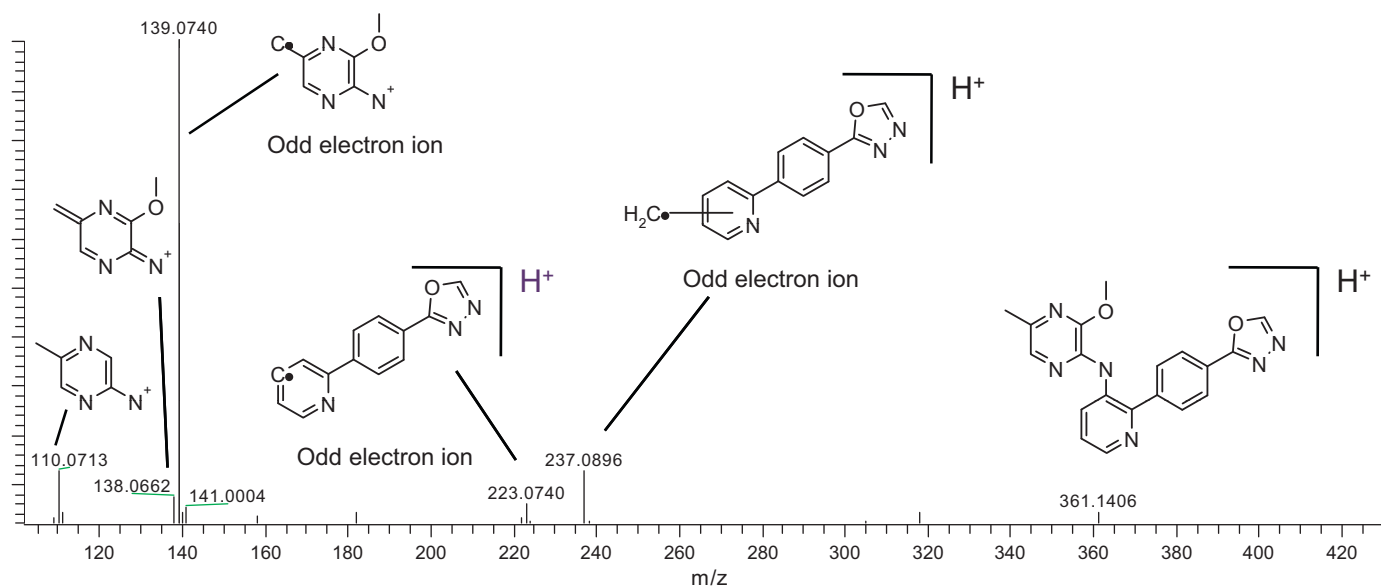


Fig. 3. Proposed fragmentation of [^{14}C]-zibotentan parent. Note: The data were generated following repeat analysis on the LTQ-Orbitrap XL for accurate mass and collision cell fragmentation data.

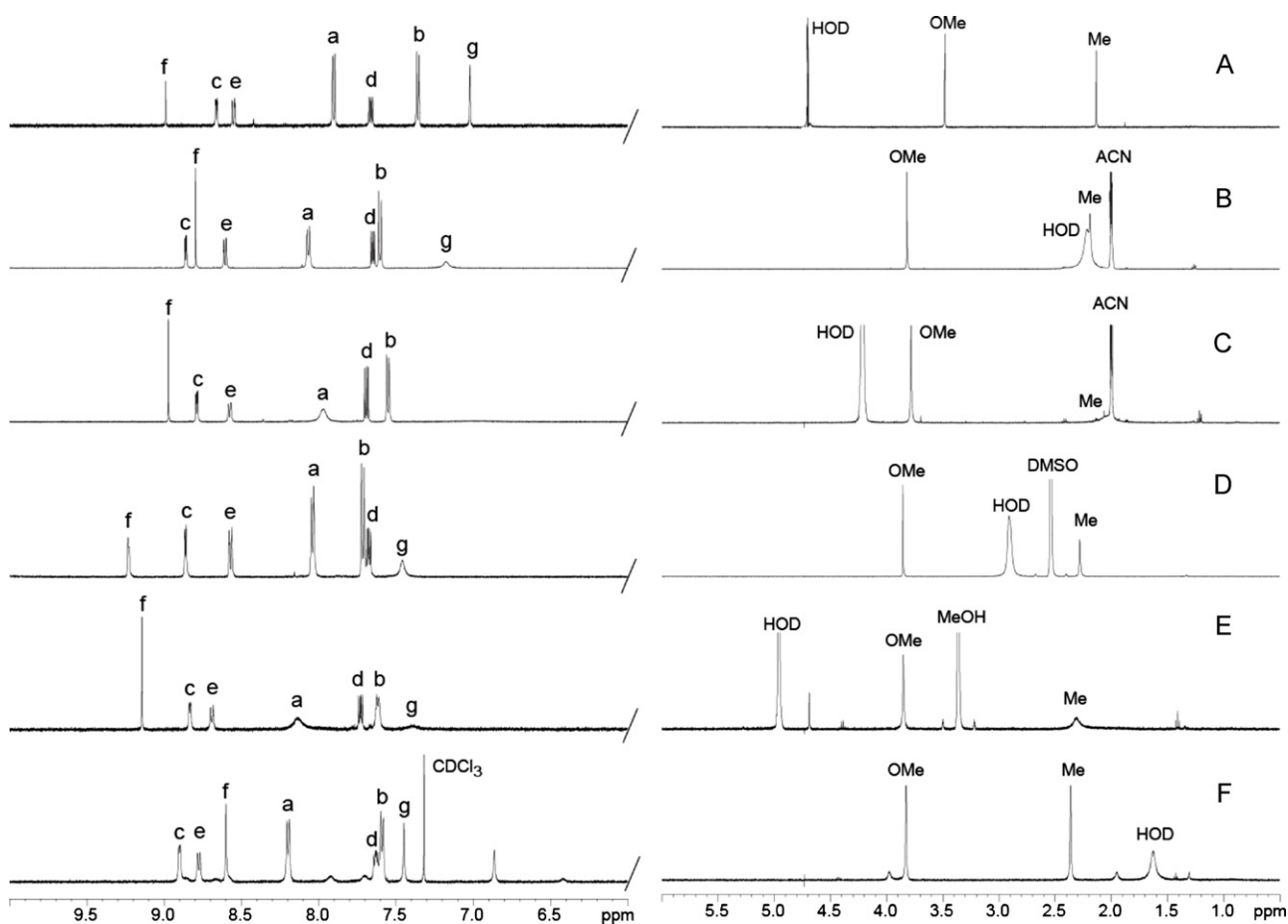


Fig. 4. ^1H NMR spectra of [^{14}C]-zibotentan in different NMR solvents. Key—A: D_2O ; B: ACN-d_3 ; C: $\text{D}_2\text{O/ACN-d}_3$ (50:50, v/v); D: DMSO-d_6 (at 100°C); E: MeOH-d_4 ; and F: CDCl_3 . Note: The aliphatic and aromatic regions are shown with different y-expansions.

The ^1H NMR spectral profile of [^{14}C]-zibotentan in D_2O (as shown in Figs. 4 and 6) comprised a singlet, representing the oxadiazole proton (labelled f) with a chemical shift $\delta^1\text{H}$ of 9.03. The para-substituted phenyl ring protons (labelled a and b) resonated at

$\delta^1\text{H}$ 7.95 and $\delta^1\text{H}$ 7.40 ($^3J=8.38\text{ Hz}$), respectively, and the pyridine protons gave rise to doublet-of-doublets at $\delta^1\text{H}$ 8.70 ($^3J=5.23\text{ Hz}$, $^4J=1.52\text{ Hz}$, for c) and $\delta^1\text{H}$ 8.51 ($^3J=8.22\text{ Hz}$, $^4J=1.52\text{ Hz}$, for e) and at $\delta^1\text{H}$ 7.71 ($^3J=8.22\text{ Hz}$ and 5.23 Hz for d). The pyrazole proton

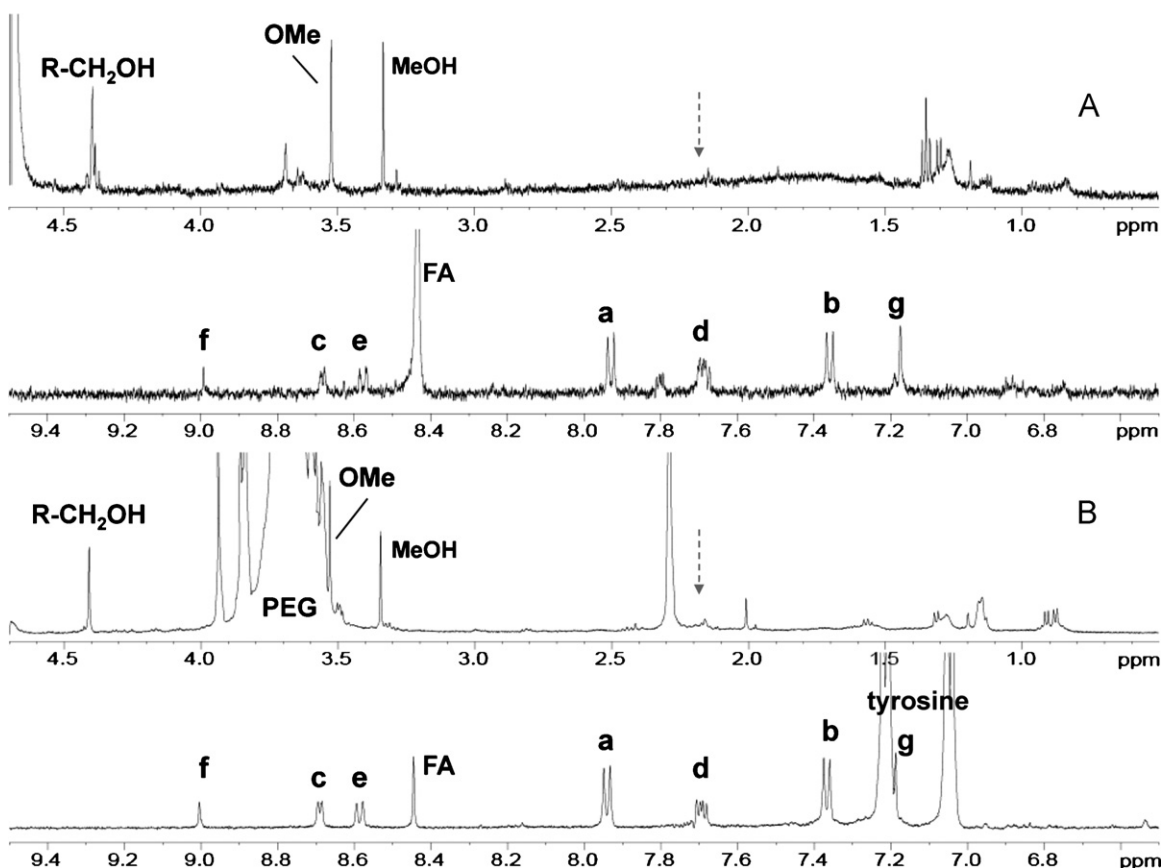


Fig. 5. Representative ^1H NMR spectra of metabolite P4 (with proton labels as shown in Fig. 1C), isolated from rat urine after oral dosing (A) and iv dosing (B). Shown are the aliphatic regions (top) and aromatic regions (bottom) for each extract. Note: The iv formulation contained PEG as dosing vehicle, which was co-extracted. FA: formic acid and MeOH: methanol, from the mobile phase used for the separation. The dashed line arrow indicates where the Me-group resonated in parent.

resonated at $\delta^1\text{H}$ 7.07 (a singlet, labelled g), while the methoxy and methyl protons resonated at $\delta^1\text{H}$ 3.52 and $\delta^1\text{H}$ 2.19, respectively.

3.2.2. Structural assignments of the major metabolites detected in rat, dog and human

As stated earlier, the main objectives of this paper were the characterisation of the major metabolites found in the excreta of rat, dog and human and the main circulating metabolites in human plasma. Hence, metabolites which were present in small amounts (<5% of dose) or were not common to all species, such as P1, P2, P5, P7, P10, P11 and P12, are not discussed.

All metabolites described below were characterised in or isolated from the rat urine samples (0–6 h collection) following dosing of single-labelled [^{14}C]-zibotentan, with the exception of P9, which was derived from the double-label rat study. All of the quantitative data, quoted below for each metabolite, however, were generated from the double-labelled studies for rat, dog and human.

Representative HPLC–RAD profiles are shown in Fig. 2, and the proposed structures and fragmentation data are summarised in Table 2.

3.2.2.1. Identification of metabolite P3. P3 was considered a major metabolite in all the species investigated. Hence, in dogs metabolite P3 represented approximately 7% of the administered dose in both urine and faeces, and ca. 5% of the radio-chromatogram in plasma. In the rat, P3 was less abundant, accounting for approximately 2% in the urines and for 1% in the faeces from male and female rats, and was not detected in the plasma samples. However, in humans

P3 represented ca. 13% of the dose in urine, yet accounted for only 2% in faeces. It was not detected as a circulating human metabolite.

Metabolite P3 (with a RT of 15.1 min) yielded a protonated molecular ion $[\text{M}+\text{H}]^+$ of m/z 303 when analysed by HPLC–MS, which is consistent with the loss of the pyrazine ring but retention of the amino sulfone moiety.

When this molecular ion was fragmented with a higher cone voltage (50 V), compound related fragments displaying the ^{14}C isotope pattern were observed at m/z 222 and m/z 286. Fragment m/z 222 related to the oxadiazole–phenyl–pyridine ring structure (the ‘aromatic backbone’) and fragment m/z 286 to the same ring structure, having retained the sulfone moiety.

Hence, P3 was identified as the despyrazine metabolite of [^{14}C]-zibotentan. The proposed structure and the fragmentation data are summarised in Table 2. The stability of sulfonamido groups, as proposed for P3, has been reported previously [15], demonstrating that chemically, this group is a relatively stable entity and can only be cleaved under harsh conditions such as strong mineral acid treatment.

The ^1H NMR spectrum of metabolite P3, isolated from rat urine indicated that whilst all of the signals from the ‘aromatic backbone’ were preserved, neither the aromatic pyrazine ring proton ($\delta^1\text{H}$ 7.0, labelled g in Fig. 4) nor the Me- or MeO-signals were detected (data not shown). Although the ^1H NMR data alone did not provide conclusive evidence (especially as the aliphatic region of the spectrum showed evidence of signal overlap with co-extracted endogenous material), it confirmed that the oxadiazole–phenyl–pyridine ring structure remained unaffected by biotransformation. This metabolite was subsequently bacterially synthesised by Novacta Biosystems Ltd., and was shown

Table 2
A summary of mass spectral data of [¹⁴C]-zibotentan and its metabolites, in order of elution, from all species investigated.

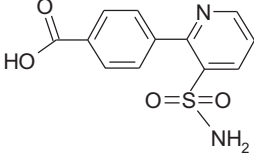
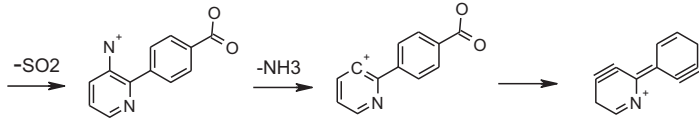
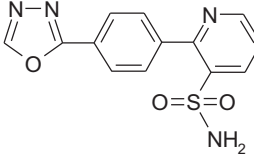
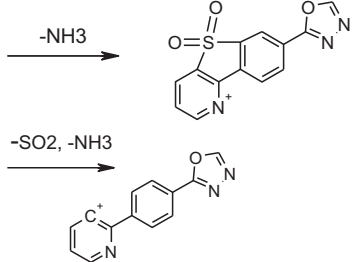
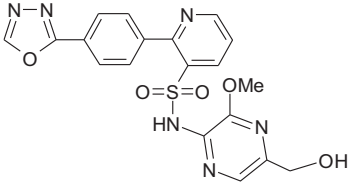
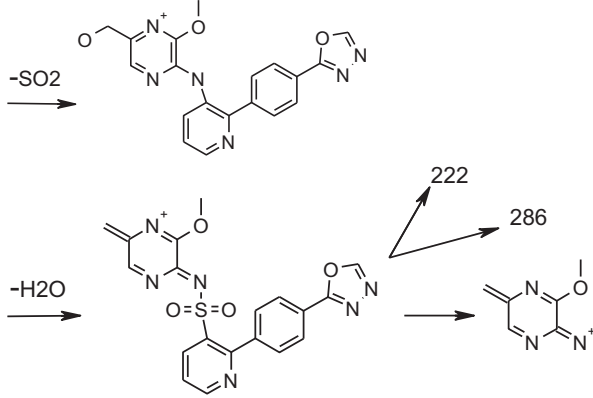
Peak label	Species	RT (min)	Proposed structure	[M+H] ⁺ (m/z)	Diagnostic fragment ions (m/z)	Proposed fragment structures
P7 ^b	R	1.9	<i>n/a</i>	-	-	-
P1 ^b	R	2.4	<i>n/a</i>	-	-	-
P12	D, H	8.4	<i>n/a</i>	-	-	-
P11	R, H	11.0	<i>n/a</i>	-	-	-
P2	R, D, H	12.5	<i>n/a</i>	-	-	-
P9 ^a	R, H	13.7		279	215, 198, 154	
P3	R, D, H	15.1		303	286	
P4	R, D, H	16.6		441	377	

Table 2 (Continued)

Peak label	Species	RT (min)	Proposed structure	[M+H] ⁺ (m/z)	Diagnostic fragment ions (m/z)	Proposed fragment structures
					155, 138	
					237	
P5	R, D, H	18.0	n/a	-	-	-
P8 ^a	R, H	20.9		401	337 and (319, 276) ^{Ref}	
					139	
					(264, 199) ^{Ref}	
Parent	R, D, H	22.1	See Fig. 3	425	361, 237, 139	
P6	R, H	23.6		441	377	
					139	

Species—detected in H: human; R: rat; and D: dog.

n/a = not available, unassigned.

^a Positively identified in repeat double-labelled study.

^{Ref} Fragments from synthetic reference standard (not seen in metabolite mass spectrum).

^b Trace metabolites eluting in solvent front.

to have the same HPLC-retention time characteristics, and produced identical MS and ^1H NMR spectra as metabolite P3 (data not shown).

3.2.2.2. Identification of metabolite P4. Generally, metabolite P4 was the most abundant metabolite detected in every biofluid and every species investigated. Hence, in male rats it represented approximately 18% of the administered dose in urine and ca. 35% in faeces. In female rats, P4 was less abundant with ca. 7% in the urine and 12% in the faeces. In plasma, it was absent in females but represented approximately 2% in males only. In the dog, P4 accounted for ca. 12% in urine and ca. 6% in faeces for both male and female dogs, although it was only detected (at ca. 6%) in the plasma from female dogs. Similarly, in humans, P4 represented ca. 12% of the dose in urine, yet accounted for only 2% in faeces. It was not detected as a circulating human metabolite.

Metabolite P4 (RT of 16.6 min) was shown to have a protonated molecular ion $[\text{M}+\text{H}]^+$ of m/z 441, indicative of a single oxidation (i.e. a gain of 16 mass units compared to parent), when analysed by HPLC–MS. The fragmentation was complex; however, the mass spectrum contained diagnostic molecular ions such as m/z 377 and m/z 155, corresponding to addition of 16 mass units to the key fragments, m/z 361 and m/z 139 as seen in the parent spectrum (Fig. 3).

The observation of the fragment ion at m/z 237, which was also present in the parent spectrum, indicated that the oxadiazole–phenyl–pyridine backbone remained intact and hence unaffected by metabolism, whilst the observation of fragment ion m/z 155 (and the subsequent loss of the hydroxyl radical to form m/z 138) suggested that oxidation had occurred on the pyrazine ring moiety. The exact site of oxidation could, however, not be confirmed; hence, this metabolite also required isolation for structural confirmation by ^1H NMR spectroscopy.

The proposed structure and fragmentations of metabolite P4 are summarised in Table 2.

Metabolite P4 was structurally identified by ^1H NMR analysis, which was carried out on four separately isolated P4 samples (isolated from 0–6 h rat urine), all of which contained different contaminants and varying amounts thereof. Although the spectral quality varied markedly, with contaminants ranging from PEG (contained in the dosing vehicle of the *iv* formulation) to endogenous urinary material (such as tyrosine or 3-hydroxyphenyl propionic acid), co-extracted during the fraction collection, the identity of the metabolite, could, however, be positively confirmed, as shown in Fig. 5.

The aromatic region generally showed less contamination, throughout; hence, all the aromatic protons could be accounted for, including the pyrazine proton (e.g. the protons labelled a–g). The signal for the methoxy group (a singlet at $\delta^1\text{H}$ 3.53) on the pyrazine ring was generally prone to overlap with impurities, yet in two of the samples it could be clearly and unambiguously identified. However, the pyrazine methyl, which in the parent resonated at $\delta^1\text{H}$ 2.2, was absent in every sample, whilst a singlet at ca. $\delta^1\text{H}$ 4.4–4.45, with an integral value of 2 protons, could be clearly observed in each of the metabolite spectra. The observed chemical shift change of the pyrazine methyl singlet was consistent with the oxidation of the methyl to a hydroxy methyl [16].

The mass spectral data and the ^1H NMR data both indicated that hydroxylation had occurred on the pyrazine ring, with ^1H NMR data confirming the formation of a hydroxy-methyl group. Hence, metabolite P4 was identified as hydroxymethyl- ^{14}C -zibotentan. A reference standard for P4 was later generated bio-synthetically as it could not be produced *via* a synthetic route. The bio-synthetic reference standard provided by Novacta Biosystems Ltd. was fully characterised and was shown to be identical to the urinary metabolite P4.

3.2.2.3. Identification of metabolite P8. Although metabolite P8 was not present in every species, it is noteworthy, as it was initially only detected and identified in the single-label rat study, based on the characteristic fragment ion m/z 139, having lost its radiolabel during metabolism. It could, therefore, only be quantified in the subsequent double-labelled studies, in rat, dog and human.

Metabolite P8 was predominantly detected in rats, although as a minor metabolite, where it represented approximately 2% and 1% in the urines and 3% and 2% in the faeces from male and female rats, respectively. It was absent in dogs and only present as a trace (1.5% in urine and <1% in faeces) in the excreta from male volunteers only.

Hence, in the initial single-label rat study, a metabolite (RT of 20.9 min) with a protonated molecular ion $[\text{M}+\text{H}]^+$ of m/z 401 was identified solely by its association with the diagnostic m/z 139 fragment. The HPLC–UV–RAD analysis had not shown a peak at this retention time, which suggested the component was not radiolabelled or had lost its radiolabel. On subjection to a higher cone voltage (50 V) the molecular ion $[\text{M}+\text{H}]^+$ of m/z 401 was fragmented to form ions of molecular mass m/z 139 (representing the amino pyrazine moiety) and m/z 337, which derived from the expulsion of the sulfone group (a loss of 64 mass units from the protonated molecular ion).

The fragmentation pattern and the lack of the ^{14}C isotope pattern in the mass spectrum of the peak indicated that metabolism had occurred on the oxadiazole ring. This finding was consistent with data generated during the preliminary mass balance study, where up to 8% of the dose was recovered in expired CO_2 following administration of ^{14}C -zibotentan to rats. Hence, the overall loss of 24 mass units compared to parent, equating to the loss of one carbon (the radiolabelled carbon) and two nitrogens, with the addition of an oxygen, suggested that metabolite P8 was the carboxylic acid metabolite of zibotentan, namely the biaryl acid metabolite.

This metabolite was subsequently confirmed in the repeat double-label rat study, where the radiolabel was positioned in the pyridine ring (as shown in Fig. 1B). Here, the HPLC–UV–RAD data of rat urine and faecal extract were similar to the single-labelled study, however, clearly demonstrating the presence of P8, eluting with a retention time of 20.9 min (Table 1 and Fig. 2A). The P8 metabolite displayed identical chromatographic retention time characteristics and HPLC–MS fragmentation patterns as the metabolite identified in the single-labelled rat study. It was also later available as a synthetic standard aiding its full characterisation by comparison of chromatographic retention time and HPLC–MS, yielding fragments of m/z 337, 319, 264, 199 and 139 (as detailed in Table 2).

3.2.2.4. Identification of metabolite P9. Similar to metabolite P8, P9 was only detected in the HPLC–UV–RAD spectrum and, therefore, quantifiable in the double-label repeat studies.

Again, it was a minor metabolite, predominantly detected in the excreta of rats, where it was present in trace amounts in the urines of male rats only (<1%), yet in the faecal samples of both sexes (at ca. 0.9% in males and 0.3% in females). It was not detected in dogs, and only present in trace amounts (<1%) in the faecal samples of the human volunteers.

Hence, the repeat double-labelled rat study revealed a peak for metabolite P9 in the HPLC–UV–RAD profile at a retention time of 13.7 min, which was identified by HPLC–MS analysis as having a protonated molecular ion $[\text{M}+\text{H}]^+$ of m/z 279. Fragmentation with a higher cone voltage (50 V) generated fragments, all displaying the ^{14}C isotope pattern, such as m/z 198, consistent with the oxadiazole ring opened carboxylic metabolite of P3, or, indeed, the despyrazine derivative of P8. Hence, P9 was identified as the despyrazine biaryl acid of ^{14}C -zibotentan.

The proposed structure for metabolite P9 and the fragmentation data are summarised in Table 2.

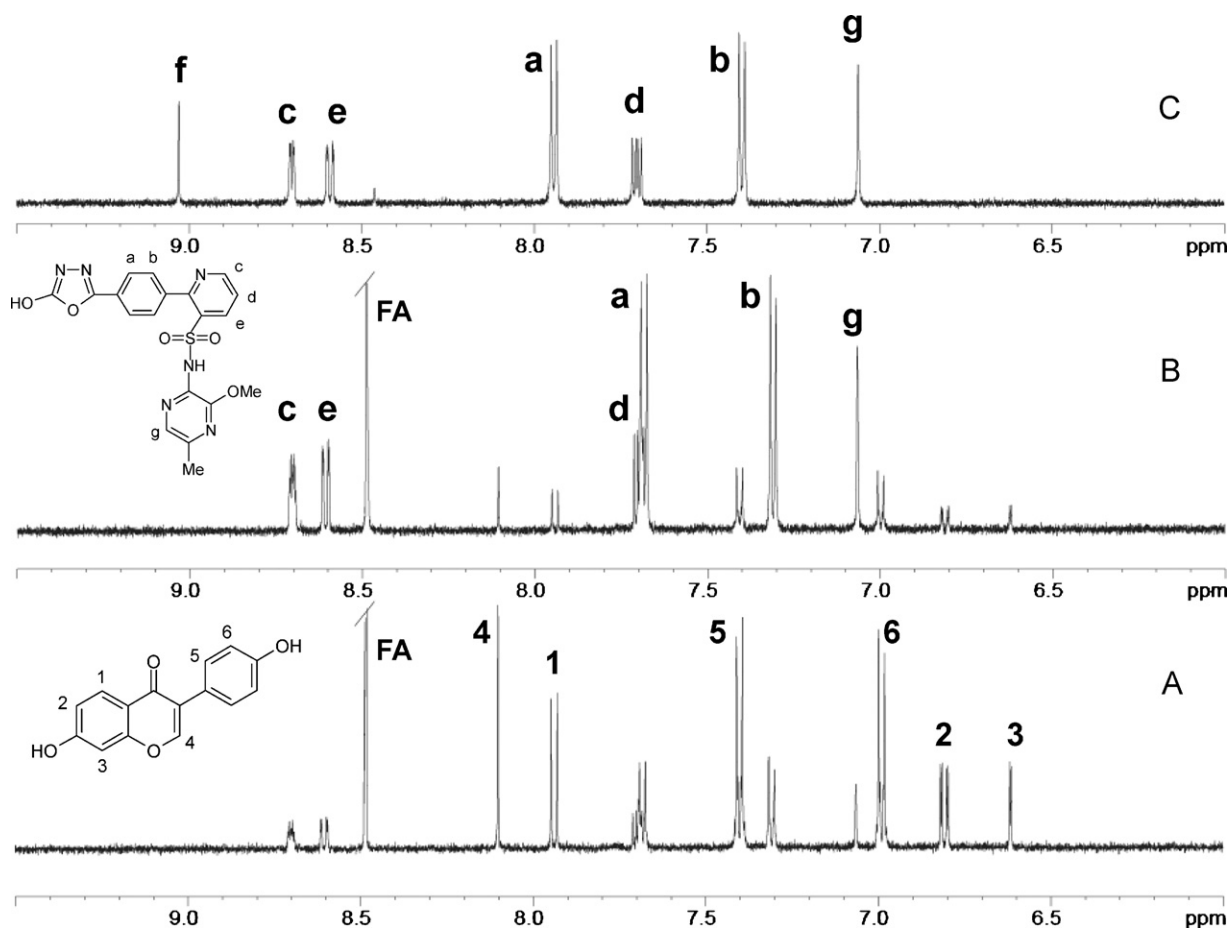


Fig. 6. The ^1H NMR spectra of [^{14}C]-zibotentan parent (C) and metabolite P6 contained in the isolated fraction B (B) and fraction A (A). Note: Only the aromatic regions are shown.

The loss of the radiolabel in the initial single-labelled study, in both metabolites P8 and P9 as a consequence of biotransformation, emphasises the importance of selecting a labelling-position unaffected by metabolism. However, as these studies have demonstrated, metabolic changes can be difficult to predict; hence, radio-labelled data should be used in conjunction with HPLC–UV–MS data, whenever possible.

3.2.2.5. Identification of metabolite P6. P6 was of particular interest as it was the only circulating metabolite (accounting for approximately 4% of the chromatogram radioactivity) detected in human plasma extracts. P6 was also detected in human urine (at approximately 5% of the dose), and in the urine and faecal samples of rat (approximately 4% and 0.5% of the administered dose, respectively). It was, however, not detected in the dog samples.

According to the FDA draft guidance on Safety Testing of Drug Metabolites (the MIST guidelines, issued in February 2008) [11], the identification of P6 was not considered mandatory, based on its low concentration in human plasma and its presence in rat excreta. Nevertheless, it was the sole plasma metabolite in humans, and a major metabolite (>5% in human urine and selected rat urine samples); hence, its full structural characterisation was desirable.

Metabolite P6 was isolated from rat urine, pooled from 12 animals. The quantity of P6 was assessed by LSC and HPLC–UV–RAD. A detailed description of the isolation of P6 is given in Section 2. To summarise briefly, multiple injections of rat urine were made onto the HPLC-column with fractions collected at 1 min intervals.

The individual fractions were then combined according to their retention times. The HPLC-separation was then repeated with the fractions of interest (at the retention time of P6) and P6 was collected manually based on the UV-response (at 259 nm), capturing the main bulk of the peak (as fraction A) and the tailing end of the UV-peak (as fraction B). Unexpectedly, LSC determined fraction A to contain ca. 16 μg , while fraction B contained approximately 31 μg . The fractions were first examined by HPLC–MS and subsequently submitted for ^1H NMR analysis.

Metabolite P6 was identified by HPLC–MS to have a protonated molecular ion $[\text{M}+\text{H}]^+$ of m/z 441 (i.e. 16 mass units over parent), indicative of a single oxidation. The fragmentation of P6 produced fragment ions of m/z 377 and m/z 139. The fragment ion at m/z 377 corresponded to addition of oxygen to the characteristic m/z 361, as seen in parent (following expulsion of the sulfone). As the m/z 139 fragment was observed, the pyrazine moiety was confirmed to have remained intact, indicating that oxidation had taken place on the oxadiazole–phenyl–pyridine moiety.

This was further substantiated by the lack of the fragment ions m/z 222, 286 and 237, which were observed in the mass spectra of P3, P4 and parent. The presence of the radioisotope pattern suggested that the oxadiazole ring radiolabel was preserved. Again, as with metabolite P4, the exact site of oxidation could not be identified based on the MS-evidence; hence, the samples (fractions A and B) were submitted for ^1H NMR spectroscopy for structural characterisation. The suggested structure and fragmentation for P6 are shown in Table 2.

Analysis of the individual HPLC-fractions (A and B) by ^1H NMR spectroscopy revealed a mixture of two components at almost

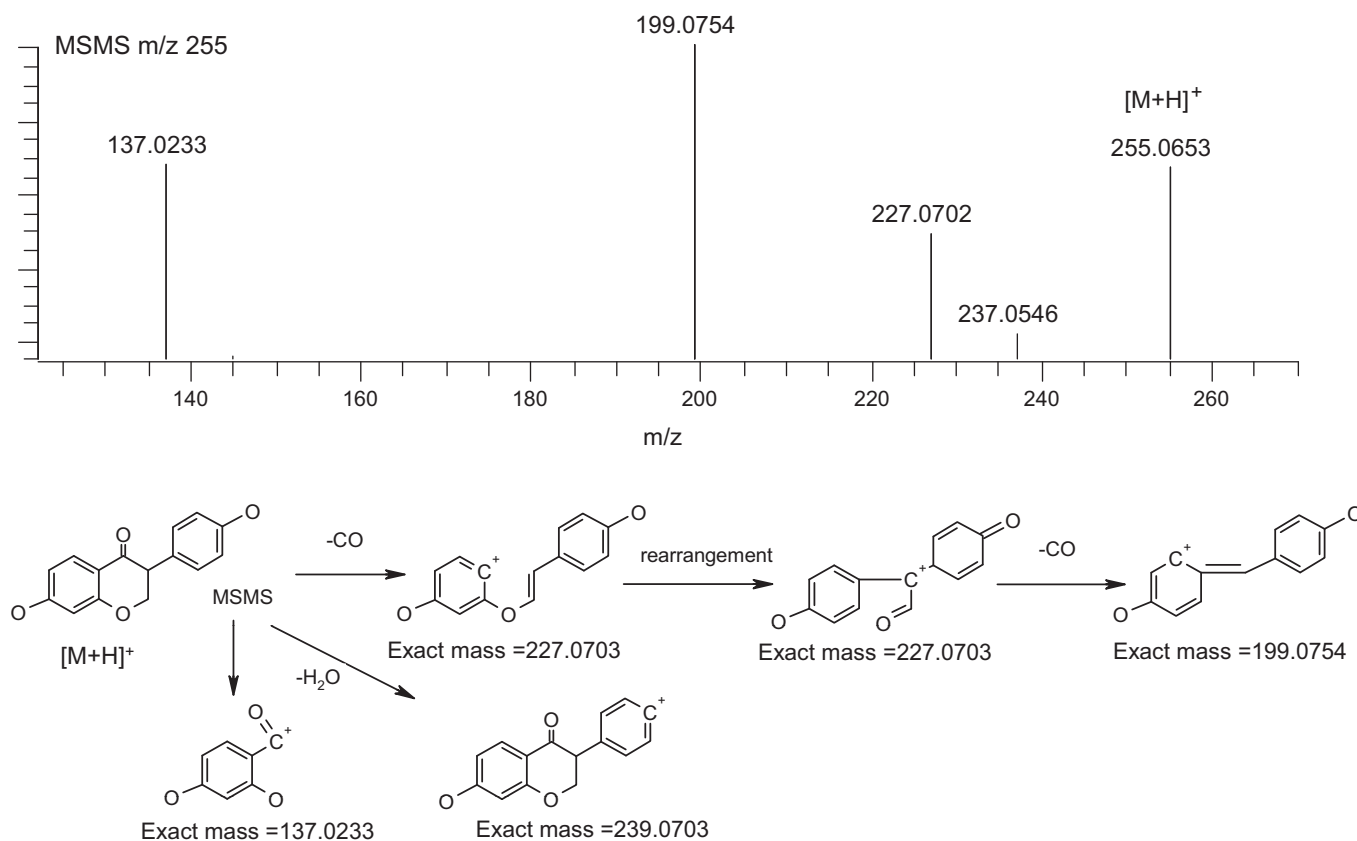


Fig. 7. LTQ-Orbitrap XL collision cell fragmentation of daidzein, the main component in fraction A, as detected in pre-dose urine [22].

equimolar concentrations (if combined). Each fraction, however, contained different proportions of each of the components, which greatly facilitated their identification.

The main component in fraction B (the tailing end of the peak, containing ca. 31 μg of P6) was identified as hydroxy- ^{14}C -zibotentan, based on the ^1H NMR spectral evidence as outlined below. The position of metabolism was confirmed to be on the oxadiazole ring as the oxadiazole proton signal ($\delta^1\text{H}$ 9.03, labelled 'f' in the parent spectrum) was not observed in the metabolite spectrum (as shown in Fig. 6), suggesting substitution with an NMR-silent moiety, such as a hydroxy-group. The residual aromatic signals were preserved, although experiencing some chemical shift changes indicative of the structural modification nearby. Hence, the protons on the para-substituted phenyl ring, in particular the protons labelled 'a', experienced a significant and characteristic chemical shift change to lower frequency (from $\delta^1\text{H}$ 7.94 to $\delta^1\text{H}$ 7.68), while the shift difference for the neighbouring signals labelled 'b' was less severe (from $\delta^1\text{H}$ 7.4 to $\delta^1\text{H}$ 7.3).

No chemical shift changes were observed for the pyridine protons (labelled c, d and e) or the pyrazole proton (labelled g). Likewise, the chemical shifts for the methoxy (OMe) and methyl (Me) signals (at $\delta^1\text{H}$ 3.53 and $\delta^1\text{H}$ 2.2, respectively) of the pyrazine moiety remained unchanged, compared to parent (part of spectrum not shown, data not shown).

The minor component contained in fraction B could be structurally evaluated in the ^1H NMR spectrum of the earlier eluting fraction (A), where it was abundant, whilst containing approximately 16 μg of metabolite P6, based on LSC data.

Hence, in the ^1H NMR spectrum of fraction A, the signals of the main component (the unknown) comprised a set of doublets from a para-substituted phenyl-ring ($\delta^1\text{H}$ 7.41 and $\delta^1\text{H}$ 7.0, with an integral value of 2 and a coupling constant of $^3J=8.4\text{ Hz}$), a singlet at

$\delta^1\text{H}$ 8.11 and a 1,3,4 substituted aromatic ring, represented by a doublet at $\delta^1\text{H}$ 7.94 ppm ($^3J=8.9\text{ Hz}$), a doublet-of-doublets at $\delta^1\text{H}$ 6.81 ($^3J=8.9\text{ Hz}$ and $^4J=2.2\text{ Hz}$) and a doublet at $\delta^1\text{H}$ 6.6 ($^4J=2.2\text{ Hz}$). There were no signals in the aliphatic region of the spectrum associated with this compound (part of spectrum not shown).

Although there were some common structural characteristics, such as the para-substituted phenyl ring, the structural resemblance to ^{14}C -zibotentan had to be ruled out on closer inspection, yet this compound warranted further investigation.

Hence, fraction A was subjected to analysis by LC-QTOF mass spectrometry. In agreement with the ^1H NMR findings the fraction was found to contain two components. The main component was determined to have an accurate mass of m/z 255.0653 Da with an elemental composition of $\text{C}_{15}\text{H}_{11}\text{O}_4$. The absence of any S or N suggested the component was not compound related, as the MSMS fragmentation exhibited no evidence of ^{14}C isotope pattern or fragments common to ^{14}C -zibotentan and detected metabolites. It had, however, also been detected in the pre-dose urine and indeed in other studies involving rat urine samples, albeit at a reduced concentration (data not shown), implying that it was an endogenous compound.

In a repeat investigation on pre-dose rat urine, using the LTQ Orbitrap, the elemental composition prediction based on an accurate mass of m/z 255.0653 Da using broad limits (i.e. maximum of 20 C, 40 H, 15 O, 15 N and 2 S, with a minimum of 0 for each element) confirmed this finding (Fig. 7).

A detailed interpretation of the accurate mass fragmentation spectra and examination of relevant literature, together with the ^1H NMR spectroscopic evidence, indicated that the compound was the flavonoid, daidzein, originating from animal feed [17–22]. The LC-MSMS spectra obtained by either the LC-QTOF or LTQ Orbitrap were shown to be identical, when comparing the rat urine sam-

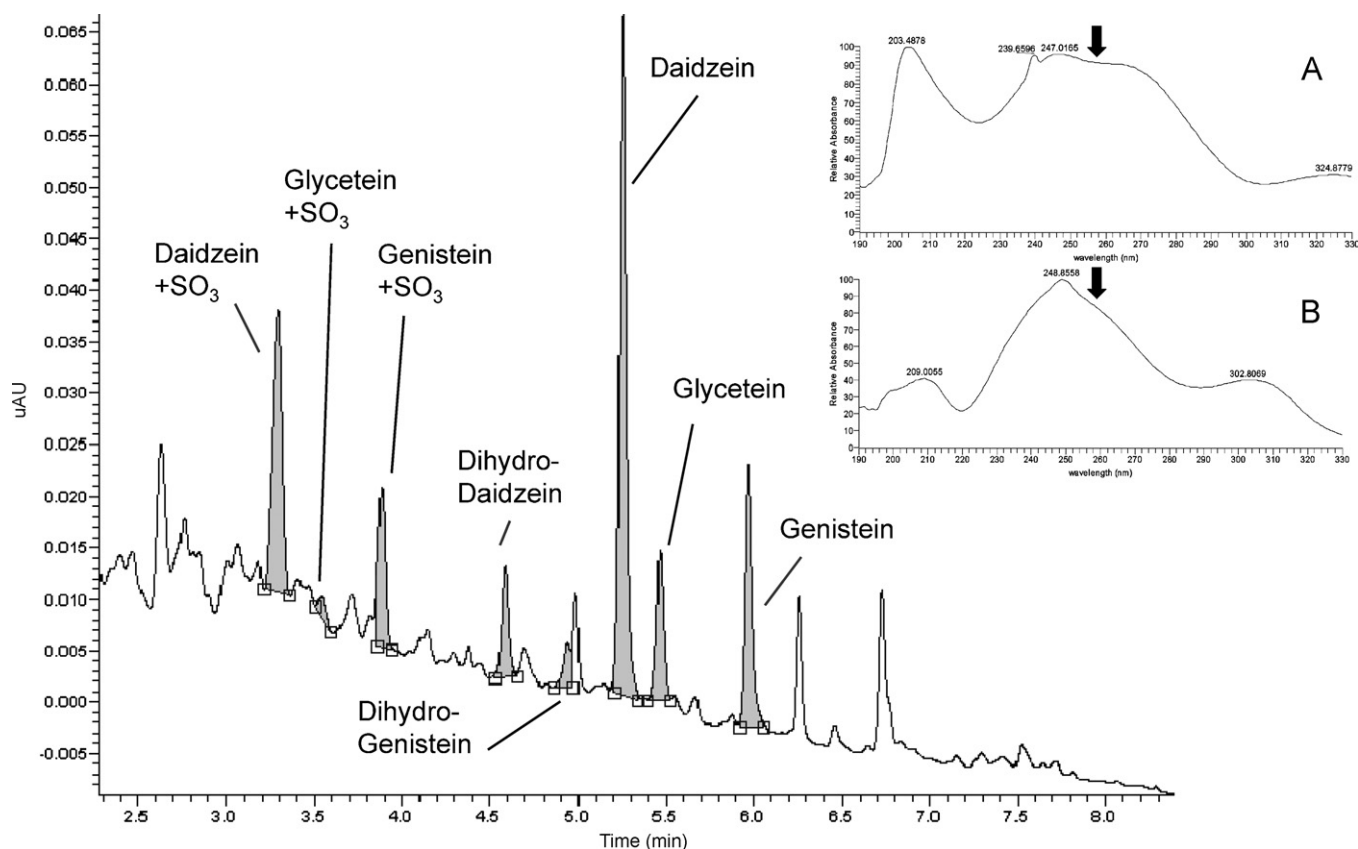


Fig. 8. Example of rat urine HPLC–UV chromatogram (300–310 nm) showing interfering peaks from excreted isoflavone components. Shown as inset are the UV absorbance traces (190–330 nm) of zibotentan (A) and daidzein (B), displaying the overlapping λ_{max} (259 nm) used in the metabolite identification of [^{14}C]-zibotentan.

ple and actual methanolic extracts from the rat pellets (data not shown). A daidzein standard was subsequently acquired to confirm the main component in fraction A and enabled the positive identification of this feed contaminant, by MS and ^1H NMR spectroscopy (data not shown).

This finding instigated additional investigations of pre-dose/control rat urine with the aim of identifying further components derived from the feed, which was available to the animals during the study. An example of a rat urine UV chromatogram (at 300–310 nm) revealing a series of components from the animal chow with MH^+ assignments is shown in Fig. 8.

Thus, several isoflavone metabolites have been identified in the rat urines (pre- and post-dose), which were shown to originate from the feed [18–22]. These included sulfate conjugates of daidzein, glycetein and genistein, the aglycones, themselves, and their dihydro-derivatives. Although the glucuronide conjugates could be easily detected by MS, they were below the limit of detection for the diode array.

The excretion of isoflavone metabolites is well documented in the literature. They are known to be derived from the soy-protein contained in the feed, where they seem to be present as glucosides. Following hydrolysis in the gut, the aglycones are then absorbed and can undergo further metabolism [18,19,21]. A summary of observed isoflavones and their respective metabolites as detected by accurate mass is presented in Table 3.

Literature data also showed that although isoflavones have been characterised by ^1H and ^{13}C NMR spectroscopy, these were generally derived from the deliberate extraction of food stuff, mainly from soybean [23–26]. In contrast, the finding presented here was from the coincidental concentration and co-extraction of daidzein,

excreted into rat urine during the metabolism study of [^{14}C]-zibotentan.

3.3. Summary

In summary, the metabolic fate of [^{14}C]-zibotentan was characterised by phase I biotransformations exclusively. It comprised the formation of the des-pyrazine metabolite P3, the hydroxylated metabolites P4 and P6 (namely the hydroxy-pyrazine and the hydroxy-oxadiazole metabolite, respectively), as well as the biaryl acid metabolites, P8 and P9, the latter being either the des-pyrazine derivative of P8 or the ring opened oxidative derivative of P3. Incubations of human urine and faecal extracts with β -glucuronidase and aryl-sulfatase confirmed that no glucuronide or sulfate conjugates were present (data not shown).

Metabolite P6 was of interest as it was the only metabolite observed in human plasma, the discovery and structural characterisation of which inadvertently led to the detection of the co-eluting and co-extracted contaminant, daidzein. Although quantification was not the key issue here, the manual collection of P6, however, relying on the UV-response alone led to the assumption that fraction A contained the majority of the metabolite, while in fact it was dominated by daidzein. The enrichment of the excreted daidzein in the sample, however, enabled its detection and characterisation by ^1H NMR spectroscopy.

Overall, the loss of radiolabel as a direct result of the biotransformation of [^{14}C]-zibotentan, coupled with the co-extraction of a compound with a similar UV-chromophore, justified the extensive efforts made to structurally elucidate and identify the unknown component, daidzein.

Table 3

A summary of accurate mass data of the observed excreted isoflavones and their respective metabolites, identified in pre-dose/control rat urine.

Name	Approximately RT (min)	[M+H] ⁺ (m/z)	Mass error (ppm)	Proposed structure
Daidzein	5.25	255.06528	0.371	
Glycetein	5.47	285.07584	0.316	
Genistein	5.97	271.06018	0.295	
Dihydro-daidzein	4.59	257.08087	0.135	
Dihydro-genistein	4.94	273.07578	0.110	
Daidzein + SO ₃	3.30	335.02194	-0.179	
Glycetein + SO ₃	3.55	365.03274	0.481	
Genistein + SO ₃	3.88	351.01683	-0.241	
Daidzein + Gluc ^a	2.78	431.09707	-0.471	
Genistein + Gluc ^a	3.03	447.09185	-0.755	

Note: Glycetein + Gluc and dihydro-glycetein were not detected.

^a Below limit of UV-detection, but identified by HPLC-MS.

As a final comment, all the metabolites presented in this paper were structurally verified and confirmed in the repeat double-labelled studies by HPLC–UV–RAD and HPLC–MS.

4. Conclusions

The investigation of [¹⁴C]-zibotentan metabolism as presented here has not been straightforward despite the presence of a radiolabel and the diversity of analytical instrumentation available.

The identification and structural characterisation of the metabolites was heavily compromised by the loss of the radiolabel due to unforeseen and unpredicted biotransformation reactions, and the importance of positioning of the radiolabel in a metabolically protected moiety has been demonstrated.

The loss of the radiolabel on the oxadiazole ring has required the repetition of the studies, using double-labelled [¹⁴C]-zibotentan, in order to capture the full range of metabolites generated and excreted. Additionally, the fragmentation was complex and unusual, yet only provided limited structural information. ¹H NMR spectroscopy was able to provide further structural characterisation, but required the isolation of every metabolite. The isolation of metabolites from complex biological matrices is a process prone to contamination due to co-elution with endogenous material and dosing vehicle, and as presented in this case, despite every effort and several HPLC-repetitions, the co-extracted isoflavone, daidzein, was observed as a major contaminant in the ¹H NMR spectrum of metabolite P6.

However, in the end, the metabolites of interest could be positively identified. Unusually, all the biotransformations were dominated by phase I reactions, such as hydroxylations, ring opened oxidations and des-alkylations, as no conjugated metabolites were observed in the study.

In summary, the metabolites structurally identified (as generally present at ca. >5% of dosed radioactivity) in human excreta and plasma were metabolites P3, P4 and P6, which were also present in the preclinical samples.

Metabolites P8 and P9 were discussed in detail as they were involved in a metabolic pathway that led to the loss of the radiolabel on the oxadiazole ring, although they did not pose a toxicity risk, being present on average at <2% of excreted radioactivity in rats and human.

All other metabolites (P1, P2, P5, P7, P11 and P12) were either only present in trace amounts in humans or excreted at <5% percentage of dose; hence, further investigations were not required.

As mentioned earlier, P6 was of particular interest, as it was the only human circulating metabolite, although it only represented ca. 4% of plasma radioactivity.

Metabolite P6 was characterised as the oxadiazole-hydroxylated-derivative of [¹⁴C]-zibotentan by ¹H NMR spectroscopy, which also revealed the presence of and led to the identification of the isoflavone, daidzein. Isoflavones are common components of soy products, which are, in turn, constituents in animal diets.

Although it has not been uncommon to detect isolated isoflavones in metabolism studies by HPLC–MS, this study, however, instigated their systematic identification in rat urine. Hence, investigations of pre-dose rat urine samples by accurate mass determination on the LTQ Orbitrap mass spectrometer revealed a series of isoflavones present as aglycones and their metabolites.

Isoflavones have previously been characterised by NMR spectroscopy predominantly in food research (mainly on soybean extracts), yet the detection of excreted urinary daidzein as a co-extracted contaminant in the ¹H NMR spectrum of P6, which was sufficiently concentrated during the sample preparation of the drug metabolite, was an unexpected discovery.

Acknowledgements

We thank Paul Phillips and Chris Smith for their support and advice in generating and interpreting the mass spectroscopy data used to determine the metabolite structures for zibotentan, and Matt Booth who was responsible for the generation, isolation and MS-structural interpretation of metabolite P3. The numerous studies involved were project managed by Dave Roberts, Mike Warwick, Alex McCormick and Ian Wilson.

References

- [1] J.W. Growcott, Preclinical anticancer activity of the specific endothelin A receptor antagonist ZD4054, *Anticancer Drugs* 20 (2009) 83–88.
- [2] N.D. James, A. Caty, M. Borre, B.A. Zonnenberg, P. Beuzeboc, T. Morris, D. Phung, N.A. Dawson, Safety and efficacy of the specific endothelin A receptor antagonist ZD4054 in patients with hormone resistant prostate cancer and bone metastases who were pain free or mildly symptomatic: a double-blind, placebo controlled, randomized, Phase II trial, *Eur. Urol.* 55 (2009) 1112–1123.
- [3] C.D. Morris, A. Rose, J. Curwen, A.M. Hughes, D.J. Wilson, D.J. Webb, Specific inhibition of the endothelin A receptor with ZD4054: clinical and pre-clinical evidence, *Br. J. Cancer* 92 (2005) 2148–2152.
- [4] E.S. Kopetz, J.B. Nelson, M.A. Carducci, Endothelin-1 as a target for therapeutic intervention in prostate cancer, *Invest. New Drugs* 20 (2002) 173–182.
- [5] W.R. Schelman, G. Liu, G. Wilding, T. Morris, D. Phung, R. Dreicer, A phase I study of zibotentan (ZD4054) in patients with metastatic, castrate-resistant prostate cancer, *Invest. New Drugs* (2009), doi:10.1007/s10637-009-9318-5 (Epub ahead of print).
- [6] H.C. Swaisland, S.D. Oliver, T. Morris, H.K. Jones, A. Bakhtyari, A. MacKee, A.D. McCormick, D. Salmon, J.A. Hargreaves, A. Millar, M.T. Taboada, In vitro metabolism of the specific endothelin-A receptor antagonist ZD4054 and clinical drug interactions between ZD4054 and rifampicin or itraconazole in healthy male volunteers, *Xenobiotica* 39 (2009) 444–456.
- [7] M. Ranson, R.H. Wilson, J.M. O'Sullivan, M. Maruoka, A. Yamaguchi, A. Cowan, J.P. Logue, H. Tomkinson, N. Tominaga, H. Swaisland, S. Oliver, M. Usami, Pharmacokinetic and tolerability profile of once-daily zibotentan (ZD4054) in Japanese and Caucasian patients with hormone-resistant prostate cancer, *Int. J. Clin. Pharmacol. Ther.* 48 (2010) 708–717.
- [8] L. Rosano, V. Di Castro, F. Spinella, S. Decandia, P.G. Natali, A. Bagnato, ZD4054, a potent endothelin receptor A antagonist, inhibits ovarian carcinoma cell proliferation, *Exp. Biol. Med.* (Maywood) 231 (2006) 1132–1135.
- [9] M. Smollich, M. Goette, J. Fischgraebe, L.F. Macedo, A. Brodie, S. Chen, I. Radke, L. Kiesel, P. Wuelfing, ETAR antagonist ZD4054 exhibits additive effects with aromatase inhibitors and fulvestrant in breast cancer therapy, and improves in vivo efficacy of anastrozole, *Breast Cancer Res. Treat.* 123 (2010) 345–357.
- [10] T.A. Baillie, M.N. Cayen, H. Fouda, R.J. Gerson, J.D. Green, S.J. Grossman, L.J. Klunk, B. LeBlanc, D.G. Perkins, L.A. Shipley, Drug metabolites in safety testing, *Toxicol. Appl. Pharmacol.* 182 (2002) 188–196.
- [11] FDA Guidance on Safety Testing of Drug Metabolites, www.fda.gov/downloads/Drugs/GuidanceComplianceRegulatoryInformation/Guidances/ucm079266.pdf (issued in February 2008).
- [12] J. Clarkson-Jones, A. Kenyon, H. Tomkinson, The disposition and metabolism of zibotentan (ZD4054), an oral specific endothelin-A receptor antagonist in mice, rats and dogs, *Xenobiotica*, accepted for publication.
- [13] J. Clarkson-Jones, A. Kenyon, J. Kemp, E.M. Lenz, S. Oliver, H. Swaisland, Metabolism and disposition of the specific endothelin A receptor antagonist zibotentan (ZD4054) in healthy volunteers, *Xenobiotica*, in press.
- [14] Z. Wang, C. Hop, M.S. Kim, S.W. Huskey, T.A. Baillie, Z. Guan, The unanticipated loss of SO₂ form sulfonamides in collision-induced dissociation, *Rapid Commun. Mass Spectrom.* 17 (2003) 81–86.
- [15] P.A. Crooks, Metabolism of sulphur-functional groups, sulphur-containing drugs and related organic compounds, in: L.A. Damani (Ed.), *Chemistry, Biochemistry and Toxicology*, vol. 1 Part B, Halsted Press, New York, 1989, pp. 183–184.
- [16] H.M. Bell, L.K. Berry, E.A. Madigan, Additive chemical shift parameters for methylene protons. Shoolery's constants reinvestigated, *Org. Magn. Reson.* 22 (1984) 693–696.
- [17] C.L. Holder, M.I. Churchwell, D.R. Doerge, Quantification of soy isoflavones, genistein and daidzein, and conjugates in rat blood using LC/ES-MS, *J. Agric. Food Chem.* 47 (1999) 3764–3770.
- [18] C.O. Cimino, S.R. Shelnut, M.J.J. Ronis, T.M. Badger, An LC–MS method to determine concentrations of isoflavones and their sulfate and glucuronide conjugates in urine, *Clin. Chim. Acta* 287 (1999) 69–82.
- [19] N. Fang, S. Yu, T.M. Badger, Characterisation of isoflavones and their conjugates in female rat urine using LC/MS/MS, *J. Agric. Food Chem.* 50 (2002) 2700–2707.
- [20] Rat diet information provided by Special Diet Services, [www.sdsdiets.com, info@sdsdiets.com](http://www.sdsdiets.com/info@sdsdiets.com).

- [21] E. Bowey, H. Adlercreutz, I. Rowland, Metabolism of isoflavones and lignans by the gut microflora: a study in germ-free and human flora associated rats, *Food Chem. Toxicol.* 41 (2003) 631–636.
- [22] F. Kuhn, M. Oehme, F. Romero, E. Abou-Mansour, R. Tabacchi, Differentiation of isomeric flavone/isoflavone aglycones by MS2 ion trap mass spectrometry and a double neutral loss of CO, *Rapid Commun. Mass Spectrom.* 17 (2003) 1941–1949.
- [23] R.P. Maskey, R.N. Asolkar, M. Speitling, V. Hoffmann, I. Gruen-Wollney, W.F. Fleck, H. Laatsch, Flavones and new isoflavone derivatives from microorganisms: isolation and structure elucidation, *Z. Naturforsch.* 58 (2003) 686–691.
- [24] J.H. Sung, S.J. Choi, S.W. Lee, K.H. Park, T.W. Moon, Isoflavones found in Korean soybean paste as 3-hydroxy-3-methylglutaryl coenzyme A reductase inhibitors, *Biosci. Biotechnol. Biochem.* 68 (2004) 1051–1058.
- [25] T.S. Chang, H.Y. Ding, S. Shou-Ku, C.Y. Wu, Metabolism of the soy isoflavones daidzein and genistein by fungi used in the preparation of various fermented soybean foods, *Biosci. Biotechnol. Biochem.* 71 (2007) 1330–1333.
- [26] A. Caligiani, G. Palla, A. Maietti, M. Cirliani, V. Brandolini, ¹H NMR fingerprinting of soybean extracts, with emphasis on identification and quantification of isoflavones, *Nutrients* 2 (2010) 280–289.